Physics Letters A 379 (2015) 157–162

Contents lists available at ScienceDirect

Physics Letters A

www.elsevier.com/locate/pla

On rotational dynamics of inertial disks in creeping shear flow

Niranjan Reddy Challabotla *, Christopher Nilsen, Helge I. Andersson

Department of Energy and Process Engineering, The Norwegian University of Science and Technology, NO-7491 Trondheim, Norway

ARTICLE INFO

Article history:
Received 16 June 2014
Received in revised form 15 October 2014
Accepted 21 October 2014
Available online 18 November 2014
Communicated by F. Porcelli

ABSTRACT

The rotational motion of an inertial disk-like particle in a creeping linear shear flow is investigated. A disk-like particle in a linear shear flow tends to rotate in the velocity-gradient plane as do rod-like particles. Unlike prolate spheroids, however, oblate spheroids always attain the same steady rotation in the shear plane irrespective of their initial orientation. The drift of the orientation of the rotation axis towards the vorticity vector consists of two qualitatively different stages. First, the wobbling drift towards rotation in the velocity-gradient plane becomes slower with increasing particle inertia, except for the least inertial spheroids. The duration of the second stage, during which the spheroid spins up to match the angular fluid velocity, becomes independent of the aspect ratio for relatively flat particles, provided that a new shape-dependent Stokes number is used.

1. Introduction

The rotational dynamics of inertial spheroidal particles crucially depends on the aspect ratio as well as the inertia of the particle. A bi-axial ellipsoid, i.e. a spheroid, is a frequently adopted model shape for non-spherical particles. The aspect ratio k, defined as the ratio between the two equal axes and the symmetry axis, distinguishes between rod-like particles (prolate spheroids with $k < 1$) and disk-like particles (oblate spheroids with $k > 1$) and $k = 1$ corresponds to spherical particles. The rotational motion of single or many rod-like particles have recently received renewed attention of which the studies reported by Mortensen et al. [1], Lundell and Carlsson [2], Bellani et al. [3], Parsa et al. [4], Andersson et al. [5], and Nilsen and Andersson [6] are relevant examples. A topical journal issue was devoted to the dynamics of anisotropic particles in turbulent flows; see Andersson and Soldati [7].

The literature reporting the rotational dynamics of disk-like particles is comparatively scarce. Although the rotational motion of disk-like particles seems to be simpler than the intricate rotation of rod-like particles, see e.g. Qi and Luo [8], the dynamics of disk-like particles still require further exploration. Anisometric particles resembling thin disks immersed in a viscous fluid are encountered in nature (e.g. seeds, human red blood cells). A great interest in the behaviour of platelets exists in biomedical research, e.g. microcirculation flow (Mody and King [9]). Thin reflective flakes are commonly used for experimental flow visualization studies; e.g. Savaş [10], Gauthier et al. [11], and Philippe et al. [12].

Analytical and numerical investigations of anisometric particles are usually based on the analytical derivations made by Jeffery [13] for tri-axial ellipsoidal particles in a creeping shear flow. Disk-like particles are thus modeled as oblate spheroids where the ratio between the two equal major axes and the minor axis is the aspect ratio $k > 1$ which is a dimensionless measure of the flatness of the spheroidal particle.

Let us first take a look at earlier findings for *massless* disk-like particles. According to the Jeffery theory, the time evolution of a unit vector $\mathbf{p}$ parallel to the particle symmetry axis is governed by

$$\frac{d\mathbf{p}}{dt} = \boldsymbol{\Omega}\cdot\mathbf{p} - \frac{k^2-1}{k^2+1}\left[\mathbf{S}\cdot\mathbf{p} - \mathbf{p}\cdot(\mathbf{p}\cdot\mathbf{S}\cdot\mathbf{p})\right]. \tag{1}$$

The direction of the unit vector $\mathbf{p}$ identifies the orientation of the axisymmetric particle and $\boldsymbol{\Omega}$ and $\mathbf{S}$ are the anti-symmetric and symmetric parts of the fluid velocity gradient tensor in the particle frame, respectively, i.e. the rate-of-rotation and rate-of-strain tensors. This equation is valid for inertia-free axisymmetric ellipsoids irrespective of whether $k < 1$ or $k > 1$; see e.g. Leal and Hinch [14] and Gauthier et al. [11]. A disk-like particle spends most of the time with $\mathbf{p}$ along the shear axis, whereas the particle orientation vector is mostly along the flow axis for a rod-like particle. These motions are in accordance with experimental studies of Goldsmith and Mason [15] in laminar Taylor–Couette flow in a coaxial cylinder apparatus.

Recent DNS studies of anisometric particles with k in the range from 0.01 to 100 in homogeneous and isotropic turbulence by Parsa et al. [4] showed that the mean square rotation rate $\langle \dot{p}_i \dot{p}_i \rangle$ of disk-like particles ($k > 1$) is much larger than for spheres ($k = 1$). This can be qualitatively understood as the additional contribution

* Corresponding author.
E-mail address: niranjan.r.challabotla@ntnu.no (N.R. Challabotla).

http://dx.doi.org/10.1016/j.physleta.2014.10.045
0375-9601/

of strain **S** to the rotation rate in Eq. (1). Disk-like particles also show some effects of alignment with the vorticity vector $2\boldsymbol{\Omega}$ although their mean square rotation rate is substantially closer to the randomly oriented case

$$\frac{\langle \dot{p}_i \dot{p}_i \rangle}{\langle \varepsilon \rangle / \nu} = \frac{1}{6} + \frac{1}{10}\left(\frac{k^2-1}{k^2+1}\right)^2 \tag{2}$$

derived from Eq. (1) than are rod-like particles. Here, ε is the energy dissipation rate $2\nu S_{ij}S_{ij}$ and ν is the kinematic viscosity of the fluid.

The orientation of disk-like particles was utilized in an experimental study of the Taylor–Couette instability by Philippe et al. [12]. A preferential orientation of the suspended clay particles (flakes) was reported. As soon as the Taylor–Couette vortices appeared, the average orientation of the particles was slightly shifted under secondary flow effect depending on their positions in the vortices. These experimental observations are consistent with the analysis of Angilella [16] who showed that a massless and infinitely thin circular disk (i.e. $k \to \infty$) has a stable equilibrium position with **p** in the shear plane and perpendicular to the velocity.

Investigations of the dynamics of *inertial* spheroids have mostly been concerned with the translational and rotational motion of prolate spheroids. Qi and Luo [8] studied the rotation of neutrally buoyant spheroids by means of lattice Boltzmann simulations. At low particle Reynolds numbers *Re* the oblate spheroid eventually spins at a constant rate around its minor axis, which is parallel to the flow vorticity vector. This state is called 'spinning'. However, a transition occurs at $Re \approx 220$ beyond which the oblate spheroid still spins about its minor axis, but the minor axis has now a finite inclination with the vorticity. This is called 'inclined spinning' and the inclination angle increases monotonically with *Re*. Yu et al. [17] called the 'spinning' mode of Qi and Luo [8] a 'log-rolling' mode and they reported a rather different critical transition Reynolds number. They also found a second transition to a 'motionless mode' not observed by Qi and Luo [8]. Huang et al. [18] used a lattice Boltzmann method to simulate neutrally buoyant spheroids in laminar Couette flow. They found that the tumbling period of an oblate spheroid increased with *Re*. In addition to the transition reported by Qi and Luo [8], they also found a second transition to the 'motionless mode' first reported by Yu et al. [17]. Einarsson et al. [19] very recently derived an asymptotic equation of motion for small Stokes numbers (modest inertia) for the orientation vector **p** valid for both prolate and oblate spheroids.

The aim of the present study is to examine the rotational dynamics of inertial disk-like particles in a creeping linear shear flow. The objective is to explore how the particle dynamics are affected by the particle shape (aspect ratio $k > 1$) and particle inertia (to be quantified by a new shape-dependent Stokes number *St*). The mathematical modeling closely follows the recent work by Lundell and Carlsson [2] in which the effect of inertia and aspect ratio on rod-like particles ($k < 1$) in creeping shear was studied. Although gravity might affect the rotational dynamics of the heavier particles ($St \gg 1$) the effect of gravity is not included in this work.

2. Problem statement

We consider the linear shear flow $u' = \kappa z'$ in the (x', z') plane. The shear rate κ is constant here, as in Lundell and Carlsson [2], whereas a time-varying shear rate was considered by Nilsen and Andersson [6]. The Reynolds number $Re = \kappa a^2/\nu \ll 1$ in order to justify the assumption of creeping fluid motion in the vicinity of the particles, i.e. that the flow is inertia-free. $2a$ is the minor axis, i.e. the symmetry axis, of the oblate spheroid whose surface is described by

$$\frac{x^2}{a^2} + \frac{y^2}{b^2} + \frac{z^2}{b^2} = 1 \tag{3}$$

in a particle frame of reference. The particle aspect ratio $k = b/a$ is thus the essential non-dimensional geometric parameter.

The Stokes number St_{LC} is defined as the ratio between the particle time scale $\tau = a^2\rho_p/\mu_f$ and the time scale κ^{-1} of the shear flow

$$St_{LC} = \frac{\kappa a^2}{\nu}\frac{\rho_p}{\rho_f} = Re\frac{\rho_p}{\rho_f}. \tag{4}$$

The Stokes number is therefore known for a given Reynolds number *Re* and particle-to-fluid density ratio ρ_p/ρ_f. This Stokes number, which is the same as that used by Lundell and Carlsson [2], does not necessarily allow physical interpretations in the same way as in turbulent flows. This is partly due to the time scale κ^{-1} of the flow, which is not representative for any dynamics. Aside from a factor 2/9 the particle time scale τ used here is the relaxation time for translational motion of a spherical particle with radius a, although it is likely that the dynamic response of a disk-like particle to changes in the flow field depends also on the orientation and shape of the particle.

3. Mathematical modelling

3.1. Kinematics

The orientation of a spheroid is represented by a quaternion

$$\mathbf{e} = [e_0\ e_1\ e_2\ e_3]^T, \tag{5}$$

which is defined by means of the Euler angles (ϕ, θ, ψ) in accordance with the *x*-convention of Goldstein [20]; see also Ref. [21]. An orthogonal rotation matrix **R** can be defined in terms of the components of the quaternion (5) as

$$\mathbf{R} = \mathbf{E}\mathbf{G}^T \tag{6}$$

where

$$\mathbf{E} = \begin{bmatrix} -e_1 & e_0 & -e_3 & e_2 \\ -e_2 & e_3 & e_0 & -e_1 \\ -e_3 & -e_2 & e_1 & e_0 \end{bmatrix} \quad \text{and}$$

$$\mathbf{G} = \begin{bmatrix} -e_1 & e_0 & e_3 & -e_2 \\ -e_2 & -e_3 & e_0 & e_1 \\ -e_3 & e_2 & -e_1 & e_0 \end{bmatrix}. \tag{7}$$

A vector $\mathbf{a}'$ in the fixed coordinate system is now related to the vector **a** in the coordinate system fixed to the particle according to $\mathbf{a}' = \mathbf{R}\mathbf{a}$. A flow field $\mathbf{u}' = \mathbf{K}\mathbf{x}'$ in the inertial system now becomes

$$\mathbf{u} = \mathbf{R}^{\mathbf{T}}\mathbf{K}\mathbf{R}\mathbf{x} \tag{8}$$

in the particle frame of reference. Here, the velocity gradient tensor **K** is $K_{ij} = \kappa\delta_{i1}\delta_{3j}$ for the present shear flow case.

3.2. Dynamics

The rotation $\boldsymbol{\omega}$ of a spheroid is governed by the non-dimensional Euler's equation

$$\mathbf{I}\cdot\dot{\boldsymbol{\omega}} + \boldsymbol{\omega}\times(\mathbf{I}\cdot\boldsymbol{\omega}) = \frac{16\pi}{3St_{LC}}\mathbf{M} \tag{9}$$

together with the time-variation (denoted by a dot) of the quaternion

$$\dot{\mathbf{e}} = \frac{1}{2}\mathbf{G}^T\boldsymbol{\omega}. \tag{10}$$

The moment of inertia for an oblate spheroid is

$$\mathbf{I} = \frac{4}{15}\pi k^2 \begin{bmatrix} 2k^2 & 0 & 0 \\ 0 & 1+k^2 & 0 \\ 0 & 0 & 1+k^2 \end{bmatrix}. \tag{11}$$

The non-dimensional torque **M** from the shearing fluid flow on a tri-axial ellipsoidal particle was originally derived by Jeffery [13]. For the axisymmetric ellipsoid (3) the Jeffery-torque simplifies to:

$$\mathbf{M} = \begin{bmatrix} 2(\beta_0+\gamma_0)^{-1}(\Omega_{zy}-\omega_x) \\ (k^2\gamma_0+\alpha_0)^{-1}\{(k^2-1)S_{xz}+(k^2+1)(\Omega_{xz}-\omega_y)\} \\ (\alpha_0+k^2\beta_0)^{-1}\{(1-k^2)S_{xy}+(1+k^2)(\Omega_{yx}-\omega_z)\} \end{bmatrix}, \tag{12}$$

where **S** and $\boldsymbol{\Omega}$ now are the non-dimensionalized fluid rate-of-strain and rate-of-rotation tensors in the particle frame-of-reference. Similarly the expressions for the non-dimensional coefficients simplify to:

$$\alpha_0 = \int_0^\infty \frac{d\lambda}{(1+\lambda)^{3/2}(k^2+\lambda)} \quad \text{and}$$

$$\beta_0 = \gamma_0 = \int_0^\infty \frac{d\lambda}{(k^2+\lambda)^2(1+\lambda)^{1/2}}, \tag{13}$$

see Gallily and Cohen [22] and Lundell and Carlsson [2]. The vector equations (9) and (10) govern the rate-of-change with time of the angular velocity $\boldsymbol{\omega}$ and the quaternion **e** and comprise seven non-linearly coupled ordinary differential equations (ODEs).

4. Analytical solution and time scale considerations

Let us first look at the rotation of an oblate spheroid about its minor axis in the flow gradient plane. Since the two semi-major axes are equal for an oblate spheroid, M_x in Eq. (12) has simplified such that the x-component of Euler's equation (9) can be solved analytically. If ω_x is initially set to zero, we obtain the analytical solution:

$$\omega_x = \Omega_{zy}\left(1 - e^{-t/\tau_{rot}}\right), \tag{14}$$

where t is dimensionless time normalized with κ^{-1}. For the simple shear flow considered in the present study, the fluid rate-of-rotation in the particle frame non-dimensionalized with the shear rate κ in the inertial frame becomes 1/2. The relaxation time τ_{rot} for rotation about the x-axis can be expressed as:

$$\tau_{rot} = \frac{\tau}{10}k^4\beta_0 \tag{15}$$

where τ_{rot} and τ are both normalized by means of the time scale κ^{-1} of the linear shear flow. The new time scale τ_{rot} in Eq. (15), which is proportional to the time scale $2\tau/9$ which characterizes the translational motion of spherical particles, exhibits a strong explicit dependence on the flatness k of the disk-like particle. Moreover, τ_{rot} also depends implicitly on the particle shape through the dimensionless coefficient β_0 defined in Eq. (13). Here the dimensional τ is as defined in conjunction with Eq. (4). Let us recall, however, that the rotational response time for spherical particles is 3/10 of the translational relaxation time $2\tau/9$, i.e. $\tau/15$; see Zhao and Andersson [23].

In view of the preceding arguments, a physically more relevant Stokes number St should be based on τ_{rot} defined in Eq. (15) rather than on τ. This gives the new Stokes number

$$St = \frac{St_{LC}}{10}k^4\beta_0 \tag{16}$$

where St_{LC} is the Stokes number already defined in Eq. (4). The Stokes number St is believed to be a better choice than St_{LC} for parameterization of the rotational dynamics of oblate spheroids since it involves the aspect ratio k explicitly and also indirectly through the shape factor β_0 defined in Eq. (13). The ratio St/St_{LC} increases monotonically from $1/15 \approx 0.07$ for spherical particles ($k = 1$) to 1.39 and 15.5 for $k = 10$ and 100, respectively.

In computer simulations of rod-like particles suspended in a turbulent flow field, a particle relaxation time based on the assumption of an isotropic particle orientation due to Shapiro and Goldenberg [24] is routinely used by, for instance, Mortensen et al. [1] and Andersson et al. [5].

5. Computed results

The two-parameter problem defined in the mathematical modelling section has been solved for Stokes numbers St in the range from 0.1 to 100 and particle aspect ratios k in the range from 1.5 to 60. It is noteworthy that the analysis is based on the Stokes number St defined in Eq. (16) rather than on the shape-independent Stokes number St_{LC} used by Lundell and Carlsson [2]. The set of ODEs (9), (10) is integrated forward in time by means of the built-in MATLAB functions ode15s and ode45; see Ref. [25]. Irrespective of Stokes number and aspect ratio, the oblate spheroid is initially positioned with its symmetry axis almost in the z'-direction so that the particle orientation vector **p** is nearly perpendicular to the fluid vorticity vector. Since the particular orientation $\phi = \theta = \psi = 0$ is neutrally stable, we considered the slightly perturbed initial orientation $\phi = 0$, $\theta = 0.001$, and $\psi = 0.001$. The effect of different initial orientations on the rotational motion is examined in Appendix A where it is shown that an oblate spheroid eventually attains the same state of steady rotation in the flow gradient plane irrespective of its initial orientation.

The trajectory of a point on the equator of a spheroidal particle is shown in Fig. 1. At $St = 1$ the modestly oblate spheroid ($k = 1.5$) to the left in Fig. 1(b) rapidly flips away from its initial orientation and rotates about its minor axis x, i.e. the symmetry axis, which gradually becomes perpendicular to the shear plane (x', z'). For the higher Stokes numbers $St = 10$ and 100, a wobbling motion of the oblate spheroid persists over a relatively long time interval until the spheroid eventually spins up and rotates in the shear plane. The behaviour of the spheroid with the least inertia in Fig. 1(a) exhibits the same trend as the most inertial spheroid in Fig. 1(d). The rotational motion of a more disk-like spheroid ($k = 10$) is displayed to the right in Fig. 1. The disk at $St = 1$ takes longer time before aligning in the flow-gradient plane in comparison with the rapid transition observed in Fig. 1(b). At higher Stokes numbers the flatter spheroids ($k = 10$) in Fig. 1(g, h) reach a steady state faster than the only modestly flat particles ($k = 1.5$) in Fig. 1(c, d).

The particle trajectories shown in Fig. 1(e) are different from the findings of Gauthier et al. [11] for non-inertial disks with $k = 10$. They found that the orientation vector **p** described a closed orbit, a so-called Jeffery-orbit, with **p** most of the time along the shear direction z'. The Jeffery-orbit of an inertia-free disk is determined by its initial conditions which are never forgotten, whereas the effect of the initial orientation is eventually forgotten by inertial disks (this essential issue is addressed in Appendix A). The differences between the trajectories found here and those in Ref. [11] are therefore due to the inclusion of particle inertia in the present case. Inertia forces the oblate spheroid towards the flow gradient plane, as is also the case for prolate spheroids (Lundell and Carlsson [2]).

The time evolution of the angular velocity ω_x about the symmetry axis and the angular velocity $\omega_{yz} \equiv (\omega_y^2 + \omega_z^2)^{1/2}$ about an axis perpendicular to the symmetry axis are shown in Fig. 2 for $St = 1$ (left) and for $St = 100$ (right) for three different aspect

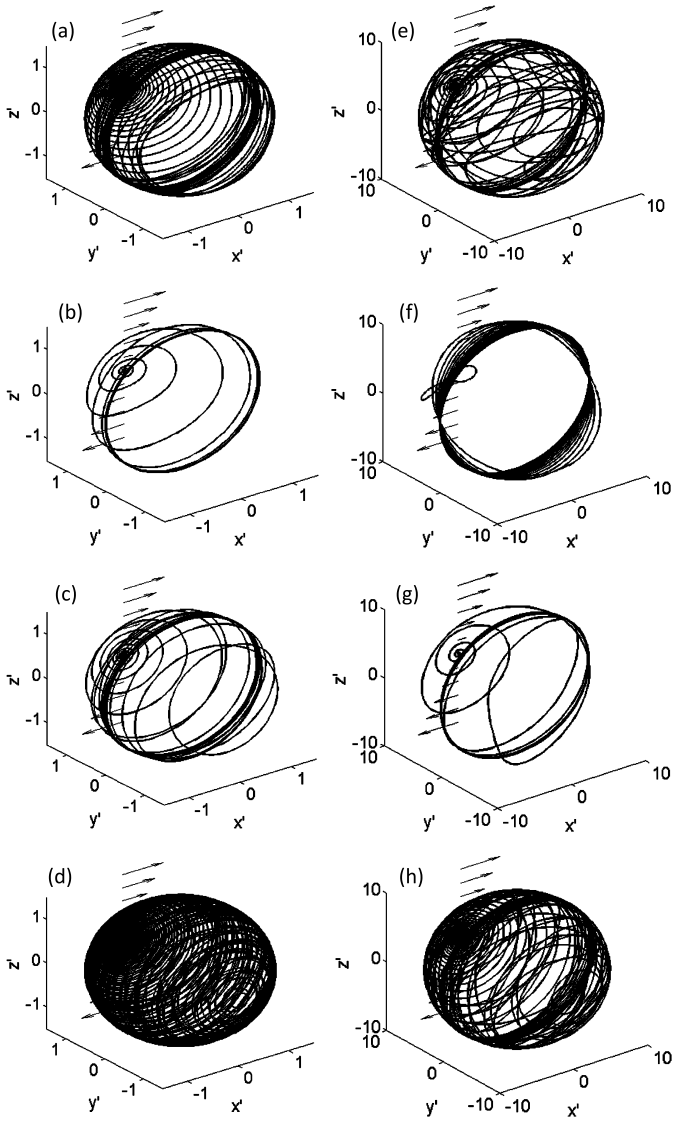

Fig. 1. Trajectory of a point on the equator of an oblate spheroid during spin-up. Aspect ratio $k = 1.5$ to the left and $k = 10$ to the right for some different Stokes numbers. $St = 0.1$ (a, e), $St = 1$ (b, f), $St = 10$ (c, g), and $St = 100$ (d, h).

ratios k. In all cases the oblate spheroid is set into rotation from its initial state $\boldsymbol{\omega} = \mathbf{0}$. During an initial stage of the particle rotation, the resultant angular velocity ω_{yz} varies periodically whereas the angular velocity about the symmetry axis $\omega_x \approx 0$. Somewhat later, however, ω_x increases monotonically towards the asymptotic limit 0.5 while ω_{yz} gradually decays to zero. These trends reflect the wobbling of the oblate spheroid before the stable rotation with the symmetry axis perpendicular to the shear-plane (x', z') and period 4π has been established. This is the same rotation period as for an inertial sphere ($k = 1$). Independent of aspect ratio k, a oblate spheroid is spun up to the same steady rotation as a spherical particle. However, a disk-like particle with only modest inertia ($St = 1.0$) approaches the flow-gradient plane more slowly as k is increased, whereas the opposite trend is observed for large inertia ($St = 100$). These trends refer to the first stage of the transient rotation during which $\omega_x \ll 0.5$. Inertia has been shown before by Lundell and Carlsson [2] to induce a drift of the particle orientation of prolate spheroids ($k < 1$) towards the flow-gradient plane and Nilsen and Andersson [6] showed that the rotation period of a prolate spheroid was crucially dependent on the Stokes number and the aspect ratio and qualitatively different from the present results for an oblate spheroid.

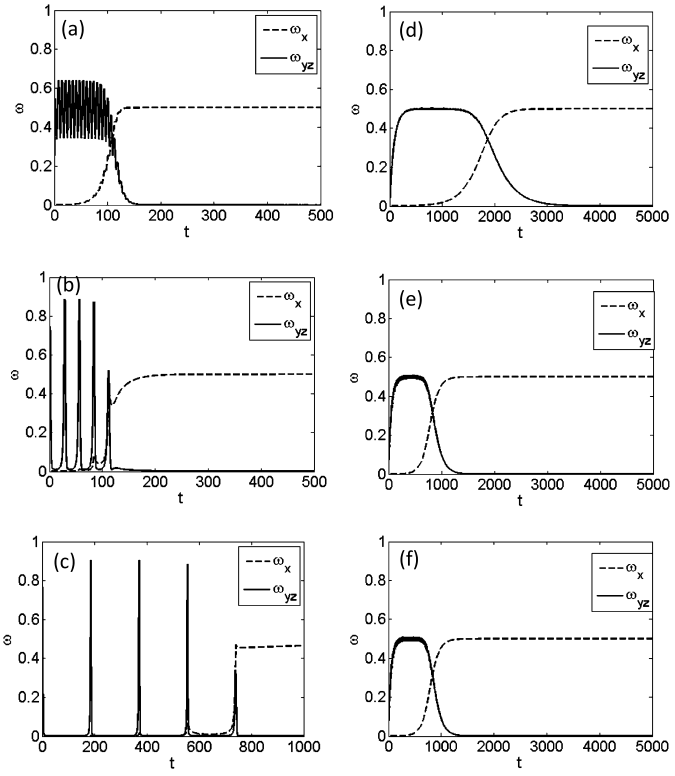

Fig. 2. Evolution of the angular velocity of an oblate spheroid during spin-up. Stokes number $St = 1.0$ to the left (panels a, b, and c) and $St = 100$ to the right (panels d, e, and f) for some different aspect ratios. $k = 1.5$ (a, d), $k = 10$ (b, e), $k = 60$ (c, f).

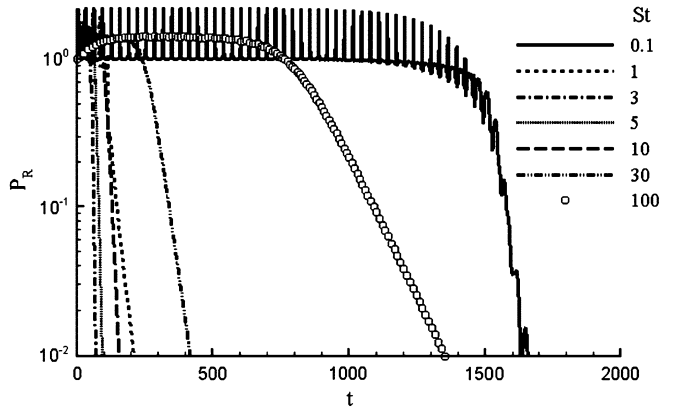

Fig. 3. Evolution of P_R with time for oblate spheroids with $k = 10$ for different Stokes numbers.

In view of the behaviour of the angular velocities in Fig. 2 we now define a rotation parameter

$$P_R = 2\left[\left(0.5 - |\omega_x|\right)^2 + \omega_y^2 + \omega_z^2\right]^{1/2} = 2\left[\left(0.5 - |\omega_x|\right)^2 + \omega_{yz}^2\right]^{1/2} \quad (17)$$

such that P_R varies from the initial value 1.0 for a non-rotating spheroid to 0 at large times when ω_x tends to either $+0.5$ or -0.5 while ω_y and ω_z approach zero. The results in Fig. 3 show how an oblate spheroid with aspect ratio $k = 10$ adjusts from the non-rotating initial condition to the ultimate state of steady rotation. The duration of the transient stage from $\boldsymbol{\omega} = \mathbf{0}$ to $\boldsymbol{\omega}_\infty = 0.5\mathbf{e}_x$ depends severely on the Stokes number. The distinctly different transient behaviour for $St = 1$ and $St = 100$ spheroids could be observed already by comparing panels (b) and (e) in Fig. 2. With increasing inertia, i.e. higher Stokes number St, the spheroid

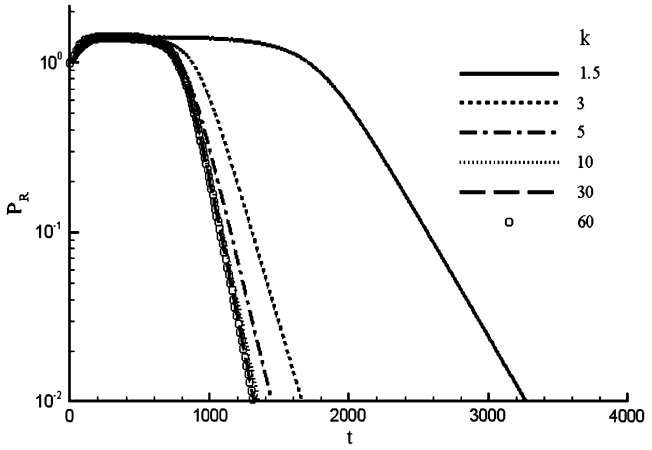

Fig. 4. Evolution of P_R with time for oblate spheroids with Stokes number $St = 100$ for different aspect ratios k.

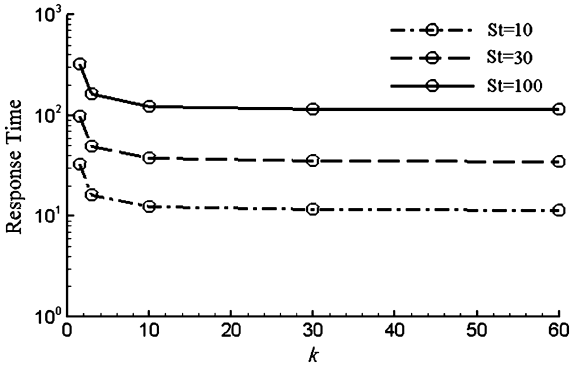

Fig. 5. Duration of the last part of the spin-up process for different aspect ratios k and three different Stokes numbers. Dotted line: $St = 10$; broken line: $St = 30$; solid line: $St = 100$.

generally requires a substantially longer time to spin up from rest and attain its ultimate steady-state rotation about its minor axis. This monotonic trend applies for $St \geq 3$. However, at the lowest Stokes number considered, i.e. $St = 0.1$, the spheroid approaches the flow-gradient plane even more slowly than the most inertial spheroid. This is attributed to the exceptionally slow growth of tiny perturbations during the first stage of the transient. After the long first stage of adaptation, the last stage of the spin-up process, during which P_R decays to zero, is short and fully in accordance with the very modest inertia of the $St = 0.1$ spheroid. It is worthwhile to recall that the time to reach the final state of rotational motion is shortest for intermediate Stokes numbers also for prolate spheroids; see Fig. 7 in Lundell and Carlsson [2].

The time evolution of the rotation parameter P_R is also shown in Fig. 4 for different particle aspect ratios k and Stokes number $St = 100$. It is readily observed that a nearly spherical spheroid ($k = 1.5$) spins up slowly and ultimately reaches the asymptotic state of steady rotation $P_R = 0$. However, the more disk-like particles, i.e. the flatter spheroids with $k > 1.5$, approach the steady rotational state substantially faster. As the aspect ratio k increases above five, the overall spin-up time seems to be independent of the aspect ratio and of the order of 1000 non-dimensional time units. It is noteworhty that this collapse of the spin-up histories for $k > 5$ at a given Stokes number has been achieved by adopting the shape-dependent Stokes number defined in Eq. (16).

Although an oblate spheroid spins up to the same ultimate state of steady rotation in the flow-gradient plane (see Appendix A), the spin-up time depends on the initial orientation of the spheroid relative to that plane, as well as on the Stokes number St and the aspect ratio k. For a given initial orientation the results displayed in Figs. 2–4 suggest that the duration of the transient period from rest to the ultimate rotation in the plane of shear consists of a first stage with unsteady rotation with $\omega_{yz}^2 \gg \omega_x^2$ and a subsequent spin-up during which ω_{yz} decays to zero and ω_x tends to $\pm 1/2$, i.e. stable rotation about the x-axis in the (x', z')-plane. The numerical solutions in Figs. 3 and 4 furthermore suggest that after the first stage with unsteady rotation the remaining approach towards the asymptotically steady state is almost exponential. Recall also the exponential evolution given by the analytical solution (14). The decay rates, i.e. the slopes in Fig. 4, increase with k. The flatter the disk, the higher the spin-up rate. The disks are rotating with non-zero components of the angular velocity vector $\boldsymbol{\omega}$ along all three directions of the particle frame of reference; see Fig. 2. The analytical solution (14) is, however, valid only if ω_x and ω_y both are zero. On the other hand, if the orientation vector $\mathbf{p}$ is initially perpendicular to the flow gradient plane (i.e. aligned with flow vorticity vector), the spin-up is truly exponential and matches the analytical solution (14). See the effect of some different initial orientations in Fig. A.1.

The duration T of this final stage of adaptation of the particle rotation can be defined as the time lapse from $P_R = 0.5$ to $P_R = 0.01$. The variation of T in the (St, k) parameter space is shown in Fig. 5. As expected, T increases with increasing inertia, i.e. higher Stokes numbers. For a given Stokes number, on the other hand, T is almost independent of the flatness of the spheroid for $k > 10$. This observation provides further support of the new shape-dependent Stokes number defined in Eq. (16). The duration T of the final spin-up process increases rapidly with decreasing flatness for $k < 10$, i.e. as the spheroid approaches spherical shape.

6. Conclusions

The rotational motion of inertial disk-like particles in creeping linear shear flow has been studied over a wide range of particle aspect ratios k and Stokes numbers St. The present study of the dynamics of oblate spheroids may therefore be considered as a sequel to the investigation by Lundell and Carlsson [2] of three-dimensional rotation of prolate spheroids in shear flow.

Starting from rest at an arbitrarily chosen initial state, a disk-like particle eventually tends to rotate in the velocity-gradient plane, as did the prolate spheroids. However, contrary to spheroidal particles with $k < 1$, the oblate spheroids with $k > 1$ rotates about their symmetry axis. The present findings for inertial spheroids are different from the observations of non-inertial spheroids by Gauthier et al. [11] who found that inertia-free disk-like particles oriented with $\mathbf{p}$, and thus the particle symmetry axis, mostly along the z'-direction. The distinctly different behaviour of the present spheroids is ascribed to particle inertia. Qi and Luo [8] studied the rotational motion of finite-sized inertial spheroids at Reynolds numbers well above unity using the lattice-Boltzmann method. Neutrally buoyant oblate spheroids with aspect ratio $k = 2$ turned out to spin up to a state of steady rotation about its minor axis with $\mathbf{p}$ aligned with the vorticity vector, i.e. in keeping with the present findings for $Re \ll 1$.

It is noteworthy that the drift of the orientation of the rotation axis towards the vorticity vector consists of two qualitatively different stages. The time scale of the first stage, in which the particle orientation changes from its arbitrary initial state to partial alignment with the vorticity vector, turns out to depend on the flatness and inertia of the disk-like particle. The last stage of the transient represents the spin-up of the axial rotation to the angular velocity of the fluid. If the particle is initially in the flow gradient plane, this spin-up is described by the analytical solution (14). In terms of a new Stokes number St based on the relaxation time τ_{rot} for rotation about the symmetry axis, as defined in Eq. (15), the duration of the spin-up stage becomes independent of particle shape

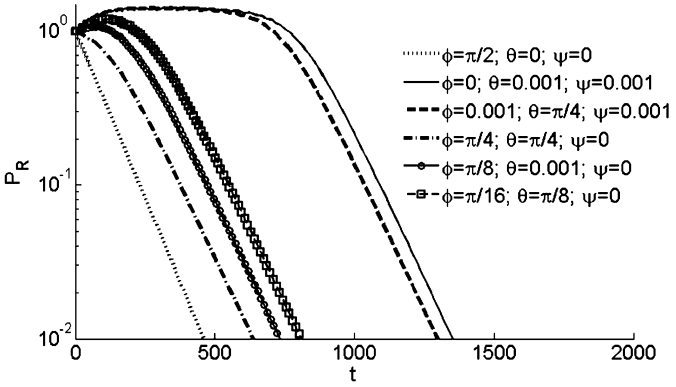

Fig. A.1. Spin-up of an inertial spheroid with $St = 100$ and $k = 10$ for six different initial orientations. The dotted line corresponds to an initial orientation with **p** perpendicular to the flow gradient plane and matches with the analytical solution (14). The solid line corresponds to the initial orientation of the oblate spheroids in Figs. 1–5.

for k greater than about 10 for a given Stokes number. Irrespective of its initial orientation, a prolate spheroid ultimately reaches the same state of steady rotation about the minor axis. The transient period required to achieve this stable steady state depends not only on the Stokes number St and the aspect ratio k but also on the initial orientation.

In a recent study of triaxial ellipsoids in linear shear flow, Lundell [26] showed that elongated ellipsoids can exhibit chaotic rotation even if they are almost axisymmetric, i.e. near-perfect prolate spheroids. On the contrary, rotation around the shortest axis of a flattened ellipsoid turned out to be stable even though they are almost axisymmetric, i.e. near-perfect oblate spheroids. Thus, compared with the prolate spheroid, the oblate spheroid has a considerable stability margin. Minute deviations from the perfect spheroidal shape do not give rise to instabilities which alter the solutions and conclusions presented in the present paper.

Acknowledgements

Funding by The Research Council of Norway through projects No. 213917/F20 “Turbulent particle suspensions” and No. 231444/F20 “Particle transport and clustering in stratified turbulence” is gratefully acknowledged. Øyvind W. Hanssen-Bauer (M.Sc.) carried out some preliminary calculations. Motivating discussions enabled by COST Action FP1005 funded by the European Science Foundation are appreciated.

Appendix A

Calculations are also performed to investigate the effect of the initial orientation of the spheroid on the rotational dynamics. The time evolutions of the rotational parameter P_R for different initial orientations are shown in Fig. A.1 for the particular parameter combination $St = 100$ and $k = 10$ case. The dotted line corresponds to a case in which the oblate spheroid is initially oriented with **p** aligned with the vorticity axis. The spheroid therefore rotates only about its minor axis, i.e. $\omega_{yz} = 0$, and asymptotically spins up to the state of steady rotation. The linear decay of P_R in the semi-logarithmic plot in Fig. A.1 is fully consistent with the exponential spin-up given by the analytical solution (14). In all other cases, in which the initial orientation of **p** is inclined with respect to the vorticity vector, the disk-like spheroid first undergoes a wobbling motion about a major axis which gradually decays to zero before the spheroid is spun up to steady rotation about its minor axis. This observation is consistent with Huang et al. [18] who recently concluded that oblate spheroid dynamics is insensitive to the initial orientation of the spheroid. It is noteworthy that exponential spin-up is observed irrespective of the initial orientation of the oblate spheroid in Fig. A.1 and, furthermore, that the spin-up rate in the final stage of spin-up process seems to be independent of the initial orientation provided that the spheroid is not oriented with **p** aligned with the fluid vorticity vector from the very beginning.

Although an oblate spheroid spins up to the same ultimate state of steady rotation in the flow-gradient plane, the overall spin-up time depends on the initial orientation of the spheroid relative to that plane, as well as on the Stokes number St and the aspect ratio k. The fastest adaptation to the rotation of the linear shear flow takes place when the spheroid is initially in the shear plane.

References

[1] P.H. Mortensen, H.I. Andersson, J.J.J. Gillissen, B.J. Boersma, Dynamics of prolate ellipsoidal particles in turbulent channel flow, Phys. Fluids 20 (2008) 093302.
[2] F. Lundell, A. Carlsson, Heavy ellipsoids in creeping shear flow: transitions of the particle rotation rate and orbit change, Phys. Rev. E 81 (2010) 016323.
[3] G. Bellani, M.L. Byron, A.G. Collignon, C.R. Meyer, E.A. Variano, Shape effects on turbulent modulation by large nearly buoyant particles, J. Fluid Mech. 712 (2012) 41–60.
[4] S. Parsa, E. Calzavarini, F. Toschi, G.A. Voth, Rotation rate of rods in turbulent fluid flow, Phys. Rev. Lett. 109 (2012) 134501.
[5] H.I. Andersson, L. Zhao, M. Barri, Torque-coupling and particle-turbulence interactions, J. Fluid Mech. 696 (2012) 319–329.
[6] C. Nilsen, H.I. Andersson, Chaotic rotation of inertial spheroids in oscillating shear flow, Phys. Fluids 25 (2013) 013303.
[7] H.I. Andersson, A. Soldati, Anisotropic particles in turbulence: status and outlook, Acta Mech. 224 (2013) 2219–2223.
[8] D. Qi, L.-S. Luo, Rotational and orientational behaviour of three-dimensional spheroidal particles in Couette flows, J. Fluid Mech. 477 (2003) 201–213.
[9] A.N. Mody, M.R. King, Three-dimensional simulations of a platelet-shaped spheroid near a wall in shear flow, Phys. Fluids 17 (2005) 113302.
[10] Ö. Savaş, On flow visualization using reflective flakes, J. Fluid Mech. 152 (1985) 235–248.
[11] G. Gauthier, P. Gondret, M. Rabaud, Motions of anisotropic particles: application to visualization of three-dimensional flows, Phys. Fluids 10 (1998) 2147–2154.
[12] A.M. Philippe, C. Baravian, M. Jenny, F. Meneau, L.J. Michot, Taylor–Couette instability in anisotropic clay suspensions measured using small-angle x-ray scattering, Phys. Rev. Lett. 108 (2012) 254501.
[13] G.B. Jeffery, The motion of ellipsoidal particles immersed in a viscous fluid, Proc. R. Soc. Lond. A 102 (1922) 161–179.
[14] L.G. Leal, E.J. Hinch, The rheology of a suspension of nearly spherical particles subject to Brownian motions, J. Fluid Mech. 55 (1972) 745–765.
[15] H.L. Goldsmith, S.G. Mason, Particle motions in sheared suspensions XIII. The spin and rotation of disks, J. Fluid Mech. 12 (1962) 88–96.
[16] J.R. Angilella, On the orientation of flat triaxial objects in shear flows, in: 2nd COST FP1005 Workshop on “Fibre Suspension Flow Modelling”, Nancy, France, 13–14 October 2011, http://www.fp1005.cism.it/presentations/nancy/JeanRegisAngilella.pdf.
[17] Z. Yu, N. Phan-Thien, R.I. Tanner, Rotation of a spheroid in a Couette flow at moderate Reynolds numbers, Phys. Rev. E 76 (2007) 026310.
[18] H. Huang, X. Yang, M. Krafczyk, X.-Y. Lu, Rotation of spheroidal particles in Couette flows, J. Fluid Mech. 692 (2012) 369–394.
[19] J. Einarsson, J.R. Angilella, B. Mehlig, Orientation dynamics of weakly inertial axisymmetric particles in steady viscous flow, Physica D 278–279 (2014) 79–85.
[20] H. Goldstein, Classical Mechanics, 2nd ed., Addison-Wesley, Reading, MA, 1980, “The Euler angles” and “Euler angles in alternate conventions”, §4-4 and Appendix B, pp. 143–148, 606–610.
[21] http://mathworld.wolfram.com/EulerAngles.html.
[22] I. Gallily, A.-H. Cohen, On the orderly nature of the motion of nonspherical aerosol particles II. Inertial collision between a spherical large droplet and an axially symmetrical elongated particle, J. Colloid Interface Sci. 68 (1979) 338–356.
[23] L. Zhao, H.I. Andersson, On particle spin in two-way coupled turbulent channel flow simulations, Phys. Fluids 23 (2011) 093302.
[24] M. Shapiro, M. Goldenberg, Deposition of glass fiber particles from turbulent air flow in a pipe, J. Aerosol Sci. 24 (1993) 65–87.
[25] http://www.mathworks.se/help/matlab/ordinary-differential-equations.html.
[26] F. Lundell, The effect of particle inertia on triaxial ellipsoids in creeping shear: from drift toward chaos to a single periodic solution, Phys. Fluids 23 (2011) 011704.